Activation of KYN-AHR axis impairs the chondrogenic and chondroprotective effects of human umbilical cord-derived mesenchymal stem cells on osteoarthritis

Yan Chang (yychang@ahmu.edu.cn)
Anhui Medical University, Ministry of Education
Xinwei Wang
Anhui Medical University, Ministry of Education
Susu Li
Anhui Medical University, Ministry of Education
Yueye Wang
Anhui Medical University, Ministry of Education
Chengyan Jia
Anhui Medical University, Ministry of Education
Xuezhi Yang
Anhui Medical University, Ministry of Education
Siyu Li
Anhui Medical University, Ministry of Education
Bingjie Zhang
Anhui Medical University, Ministry of Education
Yingjie Zhao
The Second Hospital of Anhui Medical University
Wei Wei
Anhui Medical University, Ministry of Education

Research Article

Keywords: Osteoarthritis, Human umbilical cord-derived mesenchymal stem cells, Chondrogenesis, Chondroprotective effects, AHR, Kynurenine

Posted Date: March 23rd, 2022

DOI: https://doi.org/10.21203/rs.3.rs-1440407/v1

Abstract

Background: It has been proved that intra-articular injection of mesenchymal stem cells (MSCs) could alleviate cartilage damage of osteoarthritis (OA) via differentiating into chondrocytes or protecting inherent cartilage. However, how OA articular microenvironment could affect MSCs' chondrogenic and chondroprotective efficiency has yet to be fully demonstrated. Tryptophan (Trp) metabolites, most of which are endogenous ligand for aryl hydrocarbon receptor (AHR), are abnormally increased in synovial fluid (SF) of OA patient. In this study, the effects of kynurenine (KYN), one of the most important metabolites of Trp, were evaluated on the chondrogenic and chondroprotective effects of human umbilical cord-derived mesenchymal stem cells (hUC-MSCs).

Methods: hUC-MSCs were cultured with conditioned medium containing different proportions of OA SF, then AHR activation, proliferation and chondrogenesis of hUC-MSCs were measured. In order to determine whether the chondrogenic differentiation of hUC-MSCs were regulated by AHR, hUC-MSCs were stimulated with KYN before detecting their chondrogenesis. In vitro AHR-konck down hUC-MSCs stable cell line (shAHR-UC-MSC) was generated using lentivirus transfection. Moreover, the chondroprotective effiency of shAHR-UC-MSC was determined in OA rat model.

Results: OA SF could activate AHR signaling in hUC-MSCs in a concentration-dependent manner and inhibit the chondrogenic differentiation and proliferation ability of hUC-MSCs. Similar results were observed in hUC-MSCs stimulated with KYN in vitro. AHR knockdown could remarkably eliminate the suppression effects of KYN on hUC-MSCs' chondrogenic differentiation and proliferation ability. Notably, hUC-MSCs with AHR knockdown exhibited superior therapeutic effiency in OA rat upon intra-articular injection.

Conclusion: Taken together, this study indicates that OA articular microenvironment is not conducive to the therapeutic effect of hUC-MSCs, which is related to the activation of the AHR pathway by tryptophan metabolites, thus impairs the chondrogenic and chondroprotective effects of hUC-MSCs. AHR might be a promising modification target for further improving the therapeutic efficacy of hUC-MSCs on treatment of cartilage-related diseases such as OA.

Introduction

Osteoarthritis (OA) is the most common degenerative disease of the joints through the world, with the main pathological manifestations of joint deformity and articular cartilage destruction[1]. Traditional therapeutic strategies mainly including surgeries and medical therapies. Surgical options include articular lavage, microfracture, osteochondral allograft transfer system and autologous chondrocytes implantation[2, 3], and medication treatments mainly consist of non-steroidal anti-inflammatory drugs and chondroprotective agents injection[4]. Although these interventions could alleviate the symptoms of OA and improve joint function to a certain extent, they cannot promote the regeneration of articular cartilage well and cannot fundamentally solve the destruction of articular cartilage.

Recently, with the development of cell tissue engineering, stem cells have become the new strategy and study hotspot for treatment of various diseases. MSCs, one of pluripotent stem cells, has been an ideal seed cell for the treatment of OA cartilage damage[5]. Currently, preclinical studies and clinical trials have shown that MSCs could be used to treat OA through the following ways: tissue engineering of MSCs transplantation, scaffold-free MSCs injection and MSCs exosome injection[6-8]. Although the specific mechanism of MSCs in the treatment of OA and facilitate cartilage repair is not yet clear, it may be related to the chondrogenic differentiation capacity and paracrine effects of MSCs. MSCs can differentiate into chondrocytes while recruiting resident progenitor chondrocytes at the cartilage site to promote cartilage matrix synthesis[9-11]. In addition, through paracrine effects, MSCs also secret a large number of cytokines and nutritional factors, exert anti-inflammatory and nutritional effects on damaged cartilage[12]. Although MSCs have great advantages and potential in the treatment of OA and cartilage damage, the related therapies of MSCs have not yet become clinical routine treatments[13]. As a kind of cell therapy, MSCs are susceptible to the influence of local microenvironment[14]. Some evidence suggests that the effect of MSCs therapeutics will be affected by the inflammatory environment. There is report found that the inflammatory microenvironment of acute myocardial infarction has an inhibitory effect on the stem cells potential for regenerating the injured myocardium and secretion of critical cytokines with pro-inflammatory properties cause the cellular death and hinder the stem cells proliferation and differentiation[15]. In addition, Lou found that metabolic abnormalities and the inflammatory milieu affect the differentiation potential of adipose-derived mesenchymal stem cells, impairing their functions in maintaining tissue repair and homeostasis[16].

The homeostasis of the articular microenvironment in OA is dysregulated or even disordered, therefore, it is necessary to study the influence of the articular microenvironment of OA patients on MSCs efficiency as a therapeutic agent. What's more, studies shown that the metabolic pathways for tryptophan were significantly upregulated with abnormal increased metabolites in OA patient synovial fluid[17, 18]. Tryptophan (Trp), an essential aromatic amino acid, is considered as indispensable for protein synthesis. Most of dietary Trp consumed by host is engaged in protein synthesis, while the remainder is constantly involved in Trp metabolism[19]. And the metabolites of Trp, such as kynurenine (KYN) generated under a series of endogenous enzymes or microbial metabolism, which enable to bind and activate the aryl hydrocarbon receptor (AHR), this series of process is termed the Trp-KYN-AHR pathway[20]. The activated Trp-KYN-AHR pathway can regulate a variety of physiological and pathological processes, including growth regulation, metabolism, emotions, and immunologic responses[21]. AHR is a ligand-activated nuclear transcription factor, which belongs to the Per-ARNT-Sim homology domain family member and exists in various tissues and cells[22]. Studies have shown that AHR exists in MSCs, participates in the regulation of the immune regulation process of MSCs and affects migration function and the adipogenic and osteogenic differentiation potentials of MSCs[23-25]. However, the effects of AHR on chondrogenic differentiation of MSCs still remain unclear. Due to the articular microenvironment is complicated in OA, MSCs will be exposed to SF after intra-articular injection. Whether the up-regulated Trp metabolic pathway in SF can activate AHR and affect the

chondrogenesis and chondroprotective effects of MSCs has not been reported yet, which is worth our study.

In this study, we investigated whether OA SF could activate the AHR and influence the proliferation and chondrogenic potential of human umbilical cord-derived mesenchymal stem cells (UC-MSCs). Our findings demonstrated that OA SF could activate AHR signaling pathway and inhibit chondrogenesis and proliferation of UC-MSCs, and then to investigate the role of the KYN-AHR axis in the inhibition of UC-MSCs chondrogenesis and proliferation, we used KYN to stimulate UC-MSCs at different dosages in vitro, and similar results were obtained. However, this inhibition effect was able to block by knocking down of AHR. Moreover, the complicated articular microenvironment has an unfavorable impact on UC-MSCs' chondroprotective effects, UC-MSCs with AHR knockdown had a stronger therapeutic effect on the OA rat model. These results clarified the impact of the KYN-AHR pathway on the chondrogenesis and chondroprotective effects of UC-MSCs, which provided a theoretical basis for the clinical MSCs applications in the treatment of cartilage destruction diseases such as OA.

Materials And Methods

Synovial fluid collection

Synovial fluids (SF) were obtained from healthy people (undergone total knee replacement after knee trauma), OA patients and RA patients who had undergone therapeutic arthrocentesis at the First Affiliated Hospital of Anhui Medical University. All patients have signed informed consent. SF samples were transferred to heparin-treated tubes and centrifuged at 2000 rpm for 10 min at 4 ℃ to exclude cells and debris. Then the supernatants were collected and filtered via a 0.2 μm pore size membrane to remove remaining macromolecules and stored at -80 ℃ for future use.

Cells culture

UC-MSCs (from one independent donor) were provided by Nanjing Kangya Biological Technology Co., Ltd. Cells were thawed at 37 ℃ within 1 min, then seeded into 25-cm^2 culture flasks and cultivated in Dulbecco's Modified Eagle Medium/Nutrient Mixture F-12 (DMEM/F-12, BI, Israel) containing 10% of fetal bovine serum (FBS, BI, Israel) and 1% of penicillin-streptomycin (Gibco). Cells were passaged at a split ratio of 1:3 when the confluency reached 80%. Fresh medium was replaced every 3 days, and cells between passages 3 and 6 were used in the subsequent experiments.

Phenotype of UC-MSCs

At the end of the third passage, cells were collected and washed with PBS containing 1% of bovine serum albumin (BSA; Sigma Aldrich, USA). Then, cells were resuspended with 200 μL PBS before incubating with FITC/PE/APC-conjugated mouse anti-human antibodies (CD11b, CD34, CD45, CD73, CD90 or

CD105) (Biolegend, USA) for 30 mins in the dark at 4 °C. Then, the cells were washed two times with PBS to remove unbound antibody and resuspended with 300 μL of PBS for flow cytometry analysis.

Trilineage differentiation potential of UC-MSCs

The multi-directional differentiation capabilities of UC-MSCs were detected using commercial MSCgo™ differentiation kits (BI, Israel). Briefly, UC-MSCs were seeded in a 48-well plates at the density of 1×10^4 per well and cultured with adipogenic, osteogenic, or chondrogenic differentiation induction medium. The induction medium was changed every 3 days. On day 21, cells were fixed and stained with Oil Red O for adipocytes, Alizarin Red S for osteocytes, and Alcian Blue for chondrocytes (Servicebio, China).

SF treatment

To determine the effect of SF on the chondrogenic differentiation of UC-MSCs, cells were seeded at a density of 3×10^4 cells/well in 24-well plates in the growth medium. At 80% confluence, cells were serum-starved overnight and the medium was replaced by the chondrogenic differentiation medium containing one of the following treatments: OA SF or RA SF was added to the media in a 20% or 40% ratio. The medium was replaced every 3 days, and Alcian blue staining was performed after 21 days of chondrogenic induction.

KYN treatment of UC-MSCs

To determine the effect of KYN on the chondrogenic differentiation of UC-MSCs, cells were seeded in 24-well plates with the growth medium. When the confluence is about 80%, cells were serum-starved overnight, using the chondrogenic differentiation medium containing 100 or 200 μM of KYN (Sigma, USA) to replace the medium. The medium was replaced every 3 days, and Alcian blue staining was performed after 21 days of chondrogenic induction.

Cell proliferation

The effect of SF or KYN on cell activity of UC-MSCs was measured by Cell Counting Kit 8 assay (CCK-8, Beyotime, China), cells were seeded in 96-well plates at an initial density of 1×10^3 cells/well and serum-starved overnight, then cells were cultured in DMEM/F12 containing 10% FBS and treated with SF or KYN for 7 days. At the indicated time-points (day 1, 3, 5 or 7), cells were incubated with CCK-8 solution (10 μl/well) at 37 °C for 1 h. Each time point included six replicate wells, followed by detecting the optical density at a wavelength of 450 nm by an enzyme-labeling instrument (BioTek Elx, Tecan, USA).

Lentiviral transfection

For AHR knock down, the short hairpin RNA targeting AHR (shAHR) was packaged into a lentiviral vector and constructed by Gene Chem Co. (Shanghai, China). The lentiviral vector containing a scramble sequence served as negative control (shNC). The sequences of shRNA were as below: shAHR: 5'-GCATAGAGACCGACTTAAT-3'; shNC: 5'-TTCTCCGAACGTGTCACGT-3'. Lentivirus transfection was performed following the manufacturer's instructions. The antibiotic selection which was conducted by adding puromycin (5 μg/mL, Sigma-Aldrich) and fluorescent cell sorting were employed to select stable knockdown cells.

RNA isolation and Real-time quantitative polymerase chain reaction (qRT-PCR)

According to the manufacturer's instructions to use Trizol Reagent (Thermo, USA) to extract the total RNA. The reverse transcription was performed using HiScript® II Q RT SuperMix for qRT-PCR (Vazyme Biotech, China) to synthesize cDNA. QRT-PCR was performed using AceQ® qRT-PCR SYBR Green Master Mix (Vazyme Biotech, China) on a 7500 Real-Time PCR Detection System (Applied Biosystems, USA) with gene-specific primers. Primers were synthesized by Sangon Biotech (China), the sequences of primers were as follows: AHR (forward 5'-CAGTGGTCCCAGCCTACAC-3' and reverse 5'-GACTGGCGTAGGTGATGTTG-3'), CYP1A1 (forward 5'-CTCAGTACCTCAGCAGCCAC-3' and reverse 5'-TTCTTCAGGCCTTTGGGGAC-3'), CYP1B1 (forward 5'-GACGCCTTTATCCTCTCTGCG-3' and reverse 5'-ACGACCTGATCCAATTCTGCC-3'), SOX-9 (forward 5'-GGACTTCTGAACGAGAGCGAGA-3' and reverse 5'-CGTTCTTCACCGACTTCCTCC-3'), COL2A1 (forward 5'-TGCATGAGGGCGCGGTA-3' and reverse 5'-GGTCCTGGTTGCCGGACAT-3'), Aggrecan (forward 5'-ACATTGTGGGGCTAGAACGA-3' and reverse 5'-CAGGAGGCTGCACAAGTTTT-3'), and GAPDH (forward 5'-ATGTTGCAACCGGGAAGGAA-3' and reverse 5'-AGGAAAAGCATCACCCGGAG-3'). GAPDH was regarded as a reference gene. The relative expression levels of the mRNAs in the groups were analyzed using the $2^{-\Delta\Delta CT}$ method.

Western blot analysis

The total cellular protein was obtained after lysis and the concentration of protein was measured by the BCA protein assay kit (BioChannel Biotechnology, China). The cell lysates were centrifuged and the supernatants were denatured by boiling for 10 min with 10% sodium dodecyl sulfate-polyacrylamide gel electrophoresis buffer. For Western blot, protein samples were separated by 10% SDS-polyacrylamide gel electrophoresis and transferred on polyvinylidene fluoride membrane (Millipore, USA). They then incubated with the following primary antibodies against: AHR (1:800, Santa, USA), SOX-9 (1:800, Santa, USA), COL2A1 (1:600, Proteintech, USA) and β-actin (1:10000, Cell Signaling Technology, USA). Afterwards, membranes were washed and treated with appropriate HRP-conjugated secondary antibodies and developed by electrochemiluminescence (ELC, Thermo, USA). The relative band intensity was measured using ImageJ analysis software.

Immunofluorescence staining

Cells grown on the glass coverslips were washed with ice-cold PBS, fixed with 4% formaldehyde, permeabilized with 0.2% Triton X-100, and then blocked with 5% bovine serum albumin. Then, the cells were incubated with appropriate primary antibodies at the following dilutions: anti-AHR (1:200, Santa, USA), anti-SOX-9 (1:200, Santa, USA), anti-COL2A1 (1:150, Proteintch, USA) overnight at 4 °C. The following day, cells were treated with fluorescence-labeled secondary antibodies as follows: anti-mouse IgG 488 (1:200, Biologend, USA), anti-goat IgG 594 (1:200, Biologend, USA) and anti-mouse IgG 647 (1:200, Biologend, USA) for 2 h at room temperature away from light. After PBS wash, nuclei were stained with 4',6-diamidino-2-phenylindole (DAPI, Sigma, USA) for 10 min and anti-fluorescence quencher was added. Images were taken with a confocal microscope (Leica, TCS SP8, Germany).

Alcian blue staining

To induce chondrogenic differentiation, UC-MSCs were cultured in chondrogenic differentiation medium. At day 21 after chondrogenic induction, cells were washed twice with PBS, fixed with 4% formaldehyde solution for 30 min, and stained with Alcian Blue (1% in acetic acid, pH 2.5) overnight. Then, the cells were washed 3 times with 0.1N HCL and imaged using a microscope. In addition, the content of total sulfated GAG in chondrocyte spheroids was
quantified. Briefly, chondrocyte spheroids were treated with 8 M guanidine HCL containing 0.05 M acetate, pH 5.8 and proteinase inhibitors overnight. Then, the absorbance of eluent was measured at 600 nm using a microplate reader as previously described[15].

Animal studies

All animal protocols were performed in accordance with the laboratory animal care and use guidelines and approved by the Animal Ethics Committee of institute of Clinical Pharmacology Laboratory in Anhui Medical University. 32 male Sprague-Dawley (SD) rats (approximately 12 weeks old) purchased from SPF Biotechnology Co. (Beijing, China) and housed in a specific pathogen-free (SPF) animal laboratory with 12:12 hours light/dark cycle and controlled temperature environment (23-25 °C). After 1 week of acclimatization, according to previous research[26], the rat OA model was established by completely transecting the medial collateral ligament and medial meniscus, removing the meniscus and cutting off the anterior cruciate ligament without damaging the tibial surface. After surgery, all rats received intramuscular injection of penicillin sodium (10 mg/kg) for 3 days after the operation to prevent infection. Then rats were randomly divided into four groups: (1) sham group (every rat received articular cavity injection of normal saline when the OA group was given an injection; 100 μl; n=8); (2) OA group (every rat received articular cavity injection of normal saline on the 8th week after surgery; 100 μl; n=8); (3) OA+shNC-UC-MSCs (every rat received articular cavity injection of shNC-UC-MSCs when the OA group was given an injection; 100 μl; 5×10^7 cells/mL; n=8); (4) OA+shAHR-UC-MSCs group (every rat received

articular cavity injection of shAHR-UC-MSCs when the OA group was given an injection; 100 μl; 5×10^7 cells/mL; n=8). Four weeks after injection, rats were sacrificed by and the knee samples were harvested to evaluate disease progression.

Radiography

To evaluate the severity of OA before the animals were euthanized, X-ray examination was performed on knee joint samples to observe the osteophyte formation, joint space and cartilage damage. Radiographic grading was based on Kellgren-Lawrence scoring system[27]. Radiographic scoring was performed by a single surveyor after training was provided by an experienced surgeon.

Histology and immunohistochemical analysis

After the knee joints were opened and disarticulated, the gross morphological lesions on the rat tibial plateaus were visualized and cartilage lesions and fibrillation were quantified according to the Osteoarthritis Research Society International (OARSI) guidelines[28]. Collecting knee joint samples and removing the tibiofemoral joints, the remaining femoral condyles were fixed in a neutral buffer of formalin (containing 4% formaldehyde) for 24 h. The fixed femoral condyles were decalcified in EDTA for 3 weeks and embedded in paraffin. Tissues were embedded in paraffin and sectioned into a 5-μm-thick section. The serial sections were obtained from the medial and lateral compartments at 200-μm intervals. The selected sections were deparaffinized in xylene, rehydrated through a graded series of ethanol washes, and followed by Safranin O/Fast Green staining (Servicebio, China). The cartilage degeneration was assessed by Mankin's score to assess the cartilage degeneration[29]. OARSI scoring and Mankin's scoring were performed by three independent blinded observers.

For immunohistochemistry (IHC), the deparaffinized sections were soaked in EDTA (pH 9.0) for antigen retrieval by a microwave method. The sections were placed in a 3% hydrogen peroxide solution and incubated at room temperature for 25 min in the dark, followed by blocking with 5% BSA at room temperature for 30 min. Then, the sections were incubated with primary antibody Collagen II (Abcam, UK), and Aggrecan (Abcam, UK) at 4 °C overnight, followed by the secondary antibody (Abcam, UK) at room temperature for 60 min the next day. After extensive washing, 3,3'-diaminobenzidine (DAB)-peroxidase substrate and hematoxylin solution (Servicebio, China) was added.

KYN determination in synovial fluifd by high-performance liquid chromatography (HPLC)

KYN concentrations were measured by high-performance liquid chromatography (HPLC) as previously described[30]. Briefly, frozen samples were thawed immediately prior to investigation. Protein was precipitated with trichloroacetic acid, mixed, and centrifuged at 12000 rpm and 4°C. For the

measurement, 10 µl of clear supernatant was injected into the HPLC and using Agilent TC-C18 columns (250 mm length, 5 µm grain size) for separation. Kynurenine was detected by a fluorescence detector (Agilent, G1315D) at a wavelength of 360 nm. Data were recorded by the Agilent ChemStation software.

Statistical analysis

SPSS v. 25.0 software was used for the statistical analysis, and multiple–factorial analysis of variance (ANOVA) was applied for the comparison among multiple groups. All experiments were repeated through three independent batches and results were presented as mean ± SEM, A P value < 0.05 was considered statistically significant. Cell culture samples and animals were randomly assigned to each group with about equivalent numbers in each group, and all samples were analyzed in a blinded manner.

Results

UC-MSCs identification and its characteristics

Frozen UC-MSCs were resuscitated and expanded under standard conditions. 6 h after resuscitation, cells grew with adherence and rapid proliferation. After 48 h of culture, cells reached 80% confluence with the morphology of fibroblast-like cells and spindle-shaped appearance. No noticeable variation of morphology and plastic adhesion characteristics till passage 5 (Fig. 1A).

Cell Counting Kit (CCK)-8 was used to detect the variation of proliferation activity of UC-MSCs from passage 1 and 5. The results showed no significant difference in the growth ability of UC-MSCs after 5-time passage (Fig. 1B).

Further, flow cytometry was used to identify the phenotype of UC-MSCs. The results showed that UC-MSCs were positive for the canonical MSCs markers CD73 (99.37%), CD90 (99.16%), and CD105 (99.19%) and negative for the hematopoietic markers CD11b (0.49%), CD34 (0.36%), and CD45 (0.34%) (Fig. 1C), which indicated that UC-MSCs express most of the consensus MSCs markers and suggested that these cells possess MSCs-like characteristics. Meanwhile, the differentiation potentials of UC-MSCs were also examined. As shown in Fig. 1D, oil red O, alizarin red S and alcian blue staining revealed the adipogenic, osteogenic and chondrogenic differentiation ability of UC-MSCs respectively.

RA and OA SF activated AHR and inhibited the chondrogenic and proliferative capacity of UC-MSCs

To explore the effect of SF from OA or RA patients on the chondrogenesis of UC-MSCs, UC-MSCs were cultured in chondrogenic differentiation medium plused with OA or RA SF in an indicated concentration, 0% (control), 20%, or 40% for 14 days. And apart from that, we detected the concentration

of KYN in SF from OA, RA patients, and normal donors by HPLC. Results showed that KYN was expressed at a much higher level in OA and RA patients than normal donors (Fig. S1).

Compared with the control group, the qRT-PCR analysis showed the mRNA expression of AHR and its characterized downstream target genes, including CYP1A1 and CYP1B1 was remarkably upregulated in a concentration-dependent manner (Fig. 2A), while the expression levels of SOX-9, COL2A1, and Aggrecan were significantly decreased (Fig. 2B) in SF stimulated groups. Western blot and fluorescence confocal assays consistently revealed a similar trend in protein expression (Fig. 2C-F).

milarly, extracellular matrix (ECM) secretion was also decreased in SF stimulated groups, as determined by Alcian Blue staining and quantification on day 14 (Fig. 2G, H).

We next examined the effect of SF on UC-MSCs proliferation by CCK-8 assay, as shown in Fig. 2I, treatment of UC-MSCs with OA SF or RA SF for 3, 5, and 7 days inhibited the growth abilities of UC-MSCs compared to the control group. These results indicated that OA and RA SF could activate AHR in UC-MSCs and inhibit the chondrogenesis and proliferation in UC-MSCs.

Kynurenine (KYN) treatment activated AHR and suppressed the chondrogenesis and proliferation of UC-MSCs

Previous studies have reported that, KYN, one of the tryptophan metabolites in the synovial fluid of OA and RA patients, abnormally elevated[1]. AHR is a ligand-activated nuclear transcription factor that belongs to the Per-ARNT-Sim homology domain family member, which is known to be activated by ligands, including dioxin and the IDO-derived metabolites, KYN. Upon interaction with ligands, AhR translocates to the nucleus and leads to transcription of a wide variety of genes that participate in various cellular processes. Therefore, we next used KYN to stimulate UC-MSCs and examined the nuclear translocation of AhR. We found that KYN treatment could significantly increase the translocation of AhR to the nucleus, indicating that KYN can activate AhR signaling (Fig. 3C). This result is further evidenced by the increased expression of AhR-regulated metabolic enzymes, including CYP1A1 and CYP1B1 (Fig. 6A). Moreover, to clarify whether AHR activation regulated the chondrogenesis of UC-MSCs, the chondrogenic differentiation proteims SOX-9 and COL2A1 were determined. The results of qRT-PCR found KYN significantly different doses to stimulate induced AHR, CYP1A1, and CYP1B1 gene expression in a dose-dependent manner (Fig. 3A), while inhibited the mRNA expression levels of SOX-9, COL2A1, and Aggrecan (Fig. 3B). Similarly, Western blot and immunofluorescence showed the protein expression of AHR was increased, but on the contrary, the SOX-9 and COL2A1 protein expressions were markedly reduced (Fig. 3C-F). Additionally, as shown in (Fig. 3G, H), the extracellular matrix (ECM) secretion of UC-MSCs in the KYN treatment groups was obviously suppressed compared to the control group.

CCK-8 assays were used to explore the effects of AHR activation on the proliferation of UC-MSCs, and the results indicated there was no difference in cells viability among the three groups at day 1, whereas, at

day 3, 5, and 7, the proliferation of UC-MSCs in KYN treatment groups was inhibited compared with the control group (Fig. 3I).

The establishment of sh-hUC-MSC stable cell line

The effects of AHR on chondrogenesis and proliferation were further evaluated by gene knockdown experiments using shRNA. Following puromycin selection, the knockdown efficiency was verified by the qRT-PCR, Western blot, and fluorescence staining. qRT-PCR and Western blot results showed the gene and protein expression levels of AHR in shAHR group were extremely down-regulated compared to the shNC group (Fig. 4A-C). And, fluorescent staining revealed the transfection efficiency was more than 90% (Fig. 4D). To verify whether the lentivirus changes the phenotype of UC-MSCs, flow cytometry was used to analyze the surface markers of shAHR-UC-MSCs. The results confirmed that shAHR-UC-MSCs were positive for the MSC markers CD73 (98.13%), CD90 (98.43%), and CD105 (98.79%) and negative for CD11b (0.26%), CD34 (0.69%) and CD45 (0.96%) (Fig. 4E).

AHR knockdown prevented KYN from inhibiting the chondrogenesis and proliferation of UC-MSCs

We induced the chondrogenic differentiation of UC-MSCs, shNC-UC-MSCs, and shAHR-UC-MSCs under the condition of 200 μM KYN presence. As shown in Fig. 5A, B, compared with the control group, we found KYN treatment could significantly induce the mRNA expression of AHR, CYP1A1and CYP1B1, while decreased the SOX-9, COL2A1, and Aggrecan expression in KYN and KYN+shNC-UC-MSCs groups. Whereas AHR knockdown significantly attenuated KYN-induced AHR activation and rescued SOX-9 and COL2A1 levels. Meanwhile, a similar trend of protein expression was revealed by Western blot and immunofluorescence staining (Fig. 5C-F).

Following AHR knockdown, the decreased ECM secretion of UC-MSCs induced by KYN treatment was effectively abrogated (Fig. 5G, H). Additionally, the inhibition of cell viability of UC-MSCs caused by KYN treatment was also restored after AHR knockdown (Fig. 5I)

shAHR-UC-MSCs showed a stronger chondroprotective effect on OA rats

The homeostasis of the articular microenvironment in OA is dysregulated or even disordered, whether the cartilage protective efficacy of UC-MSCs will be affected after injection into the joint cavity is unclear. Our results suggested that OA SF could affect the chondrogenesis and proliferation of UC-MSCs probably through activating the KYN-AHR axis in vivo. To investigate the role of AHR in the process of repairing cartilage damage by UC-MSCs in vivo, the surgically induced OA rat model was established, and all OA rat models received different treatments as described in the methods section. The X-ray was used to detect

the knee joint lesions and imageology results showed compared with the sham group, cartilage surface was worn and tore significantly in OA groups, and the shNC group also showed mild symptoms of joint wear (Fig. 6A). The cartilage surface was smoother in both the shAHR group and the sham group, and the joint space was more obvious compared with the OA group and the shNC group (Fig. 6A). The radiographic grading score system suggested that cartilage lesions in the OA and shNC-UC-MSCs groups were significantly higher than that of the shAHR group (Fig. 6B). The gross morphology of knee cartilage and the OARSI score exhibited the shAHR group could significantly attenuate cartilage damage and had a better therapeutic effect on cartilage regeneration than shNC groups (Fig. 6C, D). In addition, safranin-O & fast green staining showed that treatment with either shNC-UC-MSCs or shAHR-UC-MSCs could attenuate cartilage lesion and promote cartilage regeneration, while the shAHR group had more cellularity and fewer losses of the superficial layer compared with the shNC group (Fig. 6E, F). Immunohistochemistry revealed that cartilage matrix collagen II and Aggrecan expression levels in the shAHR group were more substantial than that in the shNC groups, and slightly thinner than in the sham group (Fig. 6G-J). These findings show that shAHR-UC-MSCs significantly reduced cartilage damage in the rat model and have better cartilage protection compared with shNC-UC-MSCs in the mouse OA model.

In addition, we detected the expression of Indoleamine 2,3-dioxygenase 1 (IDO1) and tryptophan 2,3-dioxygenase 2 (TDO2), both of which were rate-limiting enzyme for TRP-KYN metabolic pathway, in the synovial tissues of normal people (post trauma), OA patients, and RA patients, as well as in the synovial tissues of normal rats, OA rats, and adjuvant arthritis (AA, animal model for RA) rats. The results showed that the expressions of IDO1 and TDO2 were significantly higher in the synovial tissues of OA patients and RA patients than those of healthy control (Fig. S2A-D), and the same results could be observed in the synovial tissues of animal models (Fig. S3A-D). These results indicated that the TRP-KYN metabolic pathway were abnormally activated in joints of OA and RA patients, and the causing alternation of articular cavity microenvironment might not be supportive for the therapeutic effects of MSCs articular injection therapy.

Discussion

Osteoarthritis is one of the most prevalent joint diseases and with the characterized by articular cartilage destruction and synovitis[31]. Current main therapies are mainly attempting to relieve the symptoms and pain, but unable to have a good effect on cartilage regeneration. In recent years, with the development of cell tissue engineering technology, cell therapies based on MSCs bring OA cartilage regeneration for hopes[32, 33]. As a novel therapy for OA, although MSCs have achieved good results in preclinical studies and clinical trials, the instability of differentiation in vivo and susceptibility to pathological joint physiological microenvironment still pose challenges to the clinical applications of MSCs[34, 35]. In this study, we demonstrate that the chondrogenic efficiency of hUC-MSCs is influenced by the articular microenvironment in which they are present. OA patients' SF suppress the chondrogenic differentiation and proliferation of hUC-MSCs may through the ligand-mediated transactivation mechanism of AHR, furthermore, knocking down of AHR can block the preceding inhibition effect and improve the therapeutic efficiency of hUC-MSCs for cartilage regeneration in an OA rat model.

As a type of MSCs, hUC-MSCs have the stronger the proliferation and differentiation potential and are more appreciated in clinical practice[36], compared with other sources MSCs. In our study, hUC-MSCs have the classical MSCs characteristics and proliferate rapidly and can retain their multi-potential differentiation ability even after several passages. What's more, with the specialties of “tissue specific” regeneration[37], UC-MSCs have unlimited potential in cartilage regeneration.

It has been previously demonstrated that the therapeutic ability of MSCs for cartilage damage rely on the chondrogenic ability and paracrine effects. MSCs can differentiate into chondrocytes and induce the resident progenitor cells differentiation, and secret lots of cytokines to promote cartilage regeneration[38, 39]. However, the chondrogenic differentiation of MSCs in vivo is instable and susceptible to the microenvironment[15, 34]. The component of OA SF is complicated and may have a potential effect on chondrogenesis of MSCs, there study have showed the catabolic factors such as IL-1 or TNF-α in OA SF inhibit chondrogenesis of MSCs, but blocking IL-1 or TNF-α just partially overcame the inhibitory effect[40], which indicates that there are additional factors present in OA SF that participate in inhibition of MSCs chondrogenic differentiation. In our study, we verified that OA SF was capable of inhibiting chondrogenesis and found that OA SF impair the proliferation of hUC-MSCs besides. As the same time RA SF, as the control, also has the similar inhibitory effects on hUC-MSCs, but compared with OA SF groups, RA SF groups have stronger suppression effects which may be caused by the higher levels of pro-inflammatory cytokines[41]. And more interestingly, we also found that AHR of hUC-MSCs was activated after OA or RA SF treatment and this transactivation is in a concentration dependent manner.

AHR, a ligand-activated nuclear transcription factor, which exists in MSCs, functions as a master regulator of cell signaling pathways and participates in cell proliferation, differentiation and apoptosis[24]. With the stimulation of ligands, AHR translocate from the cytoplasm to the nucleus to regulate lower reaches gene expression, and inhibit the adipogenesis and osteogenesis of MSCs[23, 25]. The levels of tryptophan and its metabolites such as kynurenine reportedly are abnormally increased in OA SF[17, 18], kynurenine is one of the endogenous ligands of AHR. Thus, we speculated the transactivation of AHR is induced by kynurenine and involved in the inhibitory effects of OA SF on hUC-MSCs. To verify this, hUC-MSCs was were directly incubated with KYN at different dose and the results showed KYN could obviously induce the AHR activation and suppress the chondrogenesis and proliferation of hUC-MSCs.

To further confirm the role of AHR in the chondrogenic differentiation and proliferation of hUC-MSCs, we used lentivirus transfection to knock down AHR expression to obtain shAHR-hUC-MSCs and they still retained the characteristics of MSCs. In the KYN treatment experiment, the chondrogenesis and proliferation of shAHR-hUC-MSCs were significantly rescued compared with hUC-MSCs group. These results indicated that the AHR impedes the chondrogenic differentiation and proliferation in hUC-MSCs

Besides the study in vitro, an OA rat model based on knee joint instability induced by surgery, which can perfectly simulate the symptoms and pathological manifestations of human OA, was used to evaluate the effect of shAHR-hUC-MSCs in vivo. As a result, the intra-articular injection of shAHR-hUC-MSCs could

significantly attenuate cartilage damage caused by OA and had a better effect on cartilage regeneration, while the effect of shNC-hUC-MSCs was limited.

Conclusion

This study demonstrated the OA articular microenvironment is not conducive to the therapeutic effect of hUC-MSCs, which is related to the activation of the AHR pathway by tryptophan metabolites, thus impairs the chondrogenic and chondroprotective effects of hUC-MSCs. AHR might be a promising modification target for further improving the therapeutic efficacy of hUC-MSCs on treatment of cartilage-related diseases such as OA. (Fig. 7). Our findings may help in the development of more effective cartilage regeneration strategies for OA.

Abbreviations

MSCs: mesenchymal stem cells; OA: osteoarthritis; KYN: kynurenine; Trp: tryptophan; SF: synivial fluid; hUC-MSCs: human umbilical cord-derived mesenchymal stem cells; AHR: aryl hydrocarbon receptor; FBS: fetal bovine serum; MMP: matrix metalloproteinase; PBS: phosphate buffered saline; IDO: indoleamine 2,3-dioxygenase; TDO: tryptophan 2,3-dioxygenase.

Declarations

Funding

This study was supported by National Nature Science Foundation of China (No. 81573443, 82173824, 81973332, 82003763); Anhui Province Natural Science Fund (outstanding youth) (No. 170808J10); Natural Science Foundation of Anhui Provincial (No. 2108085MH320, 2108085QH383); Collaborative innovation project of key scientific research platform in Anhui Universities (No. GXXT-2020-065); The Open Fund of Key Laboratory of Antiinflammatory and Immune Medicine, Ministry of Education, P.R. China (Anhui Medical University) (No. KFJJ-2020-05); Improvement Program of Scientific Research Basement Construction (2021xkjT043); Scientific Research Fund of Anhui Medical University (No. 2020xkj026).

Conflicts of interest/Competing interests

The authors declare that they have no conflict of interest.

Ethics approval

Animals were used under the ethical approval and the ethical guidelines of the Ethics Committee of Anhui Medical University.

Consent to participate

Not applicable.

Consent for publication

Not applicable.

Availability of data and material

All data generated or analyzed during this study are included in this published article.

Code availability

Not applicable.

Authors' contributions

WW, YC and YZ performed conception and designed the study. XW, SSL, YW, CJ, XY, SYL and BZ performed most of the experiments. WW, YZ and YC analyzed the data and wrote the manuscript. All authors contributed to the article and approved the submitted version.

References

1. Hunter DJ, Bierma-Zeinstra S: **Osteoarthritis**. *Lancet*2019, **393**(10182):1745-1759.
2. Schmidt I: **Surgical Treatment Options in Thumb Carpometacarpal Osteoarthritis: A Recent Literature Overview Searching for Practice Pattern with Special Focus on Total Joint Replacement**. *Curr Rheumatol Rev*2015, **11**(1):39-46.
3. Hulme CH, Wilson EL, Peffers MJ, Roberts S, Simpson DM, Richardson JB, Gallacher P, Wright KT: **Autologous chondrocyte implantation-derived synovial fluids display distinct responder and non-responder proteomic profiles**. *Arthritis Res Ther*2017, **19**(1):150.
4. Hermann W, Lambova S, Muller-Ladner U: **Current Treatment Options for Osteoarthritis**. *Curr Rheumatol Rev*2018, **14**(2):108-116.
5. Malekpour K, Hazrati A, Zahar M, Markov A, Zekiy AO, Navashenaq JG, Roshangar L, Ahmadi M: **The Potential Use of Mesenchymal Stem Cells and Their Derived Exosomes for Orthopedic Diseases Treatment**. *Stem Cell Rev Rep*2021.
6. Lee WS, Kim HJ, Kim KI, Kim GB, Jin W: **Intra-Articular Injection of Autologous Adipose Tissue-Derived Mesenchymal Stem Cells for the Treatment of Knee Osteoarthritis: A Phase IIb, Randomized, Placebo-Controlled Clinical Trial**. *Stem Cells Transl Med*2019, **8**(6):504-511.
7. Wu J, Kuang L, Chen C, Yang J, Zeng WN, Li T, Chen H, Huang S, Fu Z, Li J*et al*: **miR-100-5p-abundant exosomes derived from infrapatellar fat pad MSCs protect articular cartilage and ameliorate gait abnormalities via inhibition of mTOR in osteoarthritis**. *Biomaterials*2019, **206**:87-100.
8. Chen X, Shi Y, Xue P, Ma X, Li J, Zhang J: **Mesenchymal stem cell-derived exosomal microRNA-136-5p inhibits chondrocyte degeneration in traumatic osteoarthritis by targeting ELF3**. *Arthritis Res*

*Ther*2020, **22**(1):256.

9. Yang Y, Lin H, Shen H, Wang B, Lei G, Tuan RS: **Mesenchymal stem cell-derived extracellular matrix enhances chondrogenic phenotype of and cartilage formation by encapsulated chondrocytes in vitro and in vivo**. *Acta Biomater*2018, **69**:71-82.
10. Diekman BO, Guilak F: **Stem cell-based therapies for osteoarthritis: challenges and opportunities**. *Curr Opin Rheumatol*2013, **25**(1):119-126.
11. Kangari P, Talaei-Khozani T, Razeghian-Jahromi I, Razmkhah M: **Mesenchymal stem cells: amazing remedies for bone and cartilage defects**. *Stem Cell Res Ther*2020, **11**(1):492.
12. Cosenza S, Ruiz M, Toupet K, Jorgensen C, Noel D: **Mesenchymal stem cells derived exosomes and microparticles protect cartilage and bone from degradation in osteoarthritis**. *Sci Rep*2017, **7**(1):16214.
13. Li N, Gao J, Mi L, Zhang G, Zhang L, Zhang N, Huo R, Hu J, Xu K: **Synovial membrane mesenchymal stem cells: past life, current situation, and application in bone and joint diseases**. *Stem Cell Res Ther*2020, **11**(1):381.
14. Lin S, Lee WYW, Feng Q, Xu L, Wang B, Man GCW, Chen Y, Jiang X, Bian L, Cui L*et al*: **Synergistic effects on mesenchymal stem cell-based cartilage regeneration by chondrogenic preconditioning and mechanical stimulation**. *Stem Cell Res Ther*2017, **8**(1):221.
15. Zhao Y, Yang X, Li S, Zhang B, Li S, Wang X, Wang Y, Jia C, Chang Y, Wei W: **sTNFRII-Fc modification protects human UC-MSCs against apoptosis/autophagy induced by TNF-alpha and enhances their efficacy in alleviating inflammatory arthritis**. *Stem Cell Res Ther*2021, **12**(1):535.
16. Louwen F, Ritter A, Kreis NN, Yuan J: **Insight into the development of obesity: functional alterations of adipose-derived mesenchymal stem cells**. *Obes Rev*2018, **19**(7):888-904.
17. Nowicka-Stazka P, Langner E, Turski W, Rzeski W, Parada-Turska J: **Quinaldic acid in synovial fluid of patients with rheumatoid arthritis and osteoarthritis and its effect on synoviocytes in vitro**. *Pharmacol Rep*2018, **70**(2):277-283.
18. Kang KY, Lee SH, Jung SM, Park SH, Jung BH, Ju JH: **Downregulation of Tryptophan-related Metabolomic Profile in Rheumatoid Arthritis Synovial Fluid**. *J Rheumatol*2015, **42**(11):2003-2011.
19. Song P, Ramprasath T, Wang H, Zou MH: **Abnormal kynurenine pathway of tryptophan catabolism in cardiovascular diseases**. *Cell Mol Life Sci*2017, **74**(16):2899-2916.
20. Sun M, Ma N, He T, Johnston LJ, Ma X: **Tryptophan (Trp) modulates gut homeostasis via aryl hydrocarbon receptor (AhR)**. *Crit Rev Food Sci Nutr*2020, **60**(10):1760-1768.
21. Labadie BW, Bao R, Luke JJ: **Reimagining IDO Pathway Inhibition in Cancer Immunotherapy via Downstream Focus on the Tryptophan-Kynurenine-Aryl Hydrocarbon Axis**. *Clin Cancer Res*2019, **25**(5):1462-1471.
22. Shinde R, McGaha TL: **The Aryl Hydrocarbon Receptor: Connecting Immunity to the Microenvironment**. *Trends Immunol*2018, **39**(12):1005-1020.

23. Heo JS, Lim JY, Pyo S, Yoon DW, Lee D, Ren WX, Lee SG, Kim GJ, Kim J: **Environmental Benzopyrene Attenuates Stemness of Placenta-Derived Mesenchymal Stem Cells via Aryl Hydrocarbon Receptor**. *Stem Cells Int*2019, **2019**:7414015.
24. Xu T, Zhou Y, Qiu L, Do DC, Zhao Y, Cui Z, Wang H, Liu X, Saradna A, Cao X*et al*: **Aryl Hydrocarbon Receptor Protects Lungs from Cockroach Allergen-Induced Inflammation by Modulating Mesenchymal Stem Cells**. *J Immunol*2015, **195**(12):5539-5550.
25. Cui Z, Feng Y, Li D, Li T, Gao P, Xu T: **Activation of aryl hydrocarbon receptor (AhR) in mesenchymal stem cells modulates macrophage polarization in asthma**. *J Immunotoxicol*2020, **17**(1):21-30.
26. Liang Y, Chen S, Yang Y, Lan C, Zhang G, Ji Z, Lin H: **Vasoactive intestinal peptide alleviates osteoarthritis effectively via inhibiting NF-kappaB signaling pathway**. *J Biomed Sci*2018, **25**(1):25.
27. Haraden CA, Huebner JL, Hsueh MF, Li YJ, Kraus VB: **Synovial fluid biomarkers associated with osteoarthritis severity reflect macrophage and neutrophil related inflammation**. *Arthritis Res Ther*2019, **21**(1):146.
28. Gerwin N, Bendele AM, Glasson S, Carlson CS: **The OARSI histopathology initiative - recommendations for histological assessments of osteoarthritis in the rat**. *Osteoarthritis Cartilage*2010, **18 Suppl 3**:S24-34.
29. Moody HR, Heard BJ, Frank CB, Shrive NG, Oloyede AO: **Investigating the potential value of individual parameters of histological grading systems in a sheep model of cartilage damage: the Modified Mankin method**. *J Anat*2012, **221**(1):47-54.
30. Venkateswaran N, Lafita-Navarro MC, Hao YH, Kilgore JA, Perez-Castro L, Braverman J, Borenstein-Auerbach N, Kim M, Lesner NP, Mishra P*et al*: **MYC promotes tryptophan uptake and metabolism by the kynurenine pathway in colon cancer**. *Genes Dev*2019, **33**(17-18):1236-1251.
31. Abramoff B, Caldera FE: **Osteoarthritis: Pathology, Diagnosis, and Treatment Options**. *Med Clin North Am*2020, **104**(2):293-311.
32. Maumus M, Guerit D, Toupet K, Jorgensen C, Noel D: **Mesenchymal stem cell-based therapies in regenerative medicine: applications in rheumatology**. *Stem Cell Res Ther*2011, **2**(2):14.
33. Su P, Tian Y, Yang C, Ma X, Wang X, Pei J, Qian A: **Mesenchymal Stem Cell Migration during Bone Formation and Bone Diseases Therapy**. *Int J Mol Sci*2018, **19**(8).
34. Kusuma GD, Carthew J, Lim R, Frith JE: **Effect of the Microenvironment on Mesenchymal Stem Cell Paracrine Signaling: Opportunities to Engineer the Therapeutic Effect**. *Stem Cells Dev*2017, **26**(9):617-631.
35. Bogdanowicz DR, Lu HH: **Designing the stem cell microenvironment for guided connective tissue regeneration**. *Ann N Y Acad Sci*2017, **1410**(1):3-25.
36. Xie Q, Liu R, Jiang J, Peng J, Yang C, Zhang W, Wang S, Song J: **What is the impact of human umbilical cord mesenchymal stem cell transplantation on clinical treatment?** *Stem Cell Res Ther*2020, **11**(1):519.
37. Fan CG, Zhang QJ, Zhou JR: **Therapeutic potentials of mesenchymal stem cells derived from human umbilical cord**. *Stem Cell Rev Rep*2011, **7**(1):195-207.

38. Mianehsaz E, Mirzaei HR, Mahjoubin-Tehran M, Rezaee A, Sahebnasagh R, Pourhanifeh MH, Mirzaei H, Hamblin MR: **Mesenchymal stem cell-derived exosomes: a new therapeutic approach to osteoarthritis?** *Stem Cell Res Ther*2019, **10**(1):340.

39. Ham O, Lee CY, Kim R, Lee J, Oh S, Lee MY, Kim J, Hwang KC, Maeng LS, Chang W: **Therapeutic Potential of Differentiated Mesenchymal Stem Cells for Treatment of Osteoarthritis**. *Int J Mol Sci*2015, **16**(7):14961-14978.

40. Takeshita M, Suzuki K, Kondo Y, Morita R, Okuzono Y, Koga K, Kassai Y, Gamo K, Takiguchi M, Kurisu R*et al*: **Multi-dimensional analysis identified rheumatoid arthritis-driving pathway in human T cell**. *Ann Rheum Dis*2019, **78**(10):1346-1356.

41. Punzi L, Pozzuoli A, Pianon M, Bertazzolo N, Oliviero F, Scapinelli R: **Pro-inflammatory interleukins in the synovial fluid of rheumatoid arthritis associated with joint hypermobility**. *Rheumatology (Oxford)*2001, **40**(2):202-204.

Figures

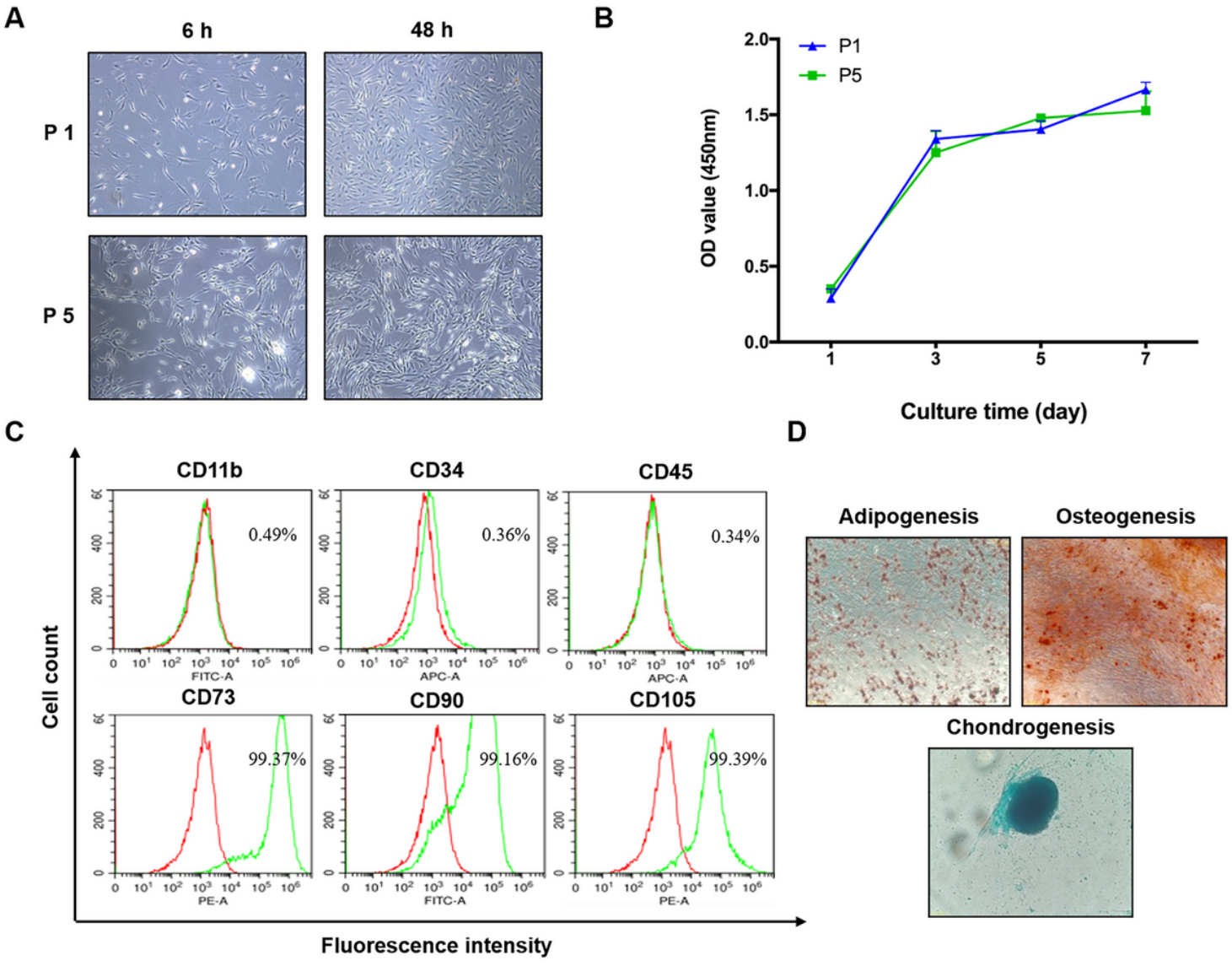

Figure 1

Identification of UC-MSCs. A Growth and morphology of UC-MSCs at 1st (P 1) and 5th passages (P 5) respectively. (scale bar = 500 μm). **B** Cell proliferation of P1 and P5 was assessed by the CCK-8 assay (n = 3). **C** The markers for UC-MSCs were detected by flow cytometry and UC-MSCs were positive for CD73, CD90 and CD105, while negative for CD11b, CD34 and CD45 (n = 3). **D** Differentiation potentials of UC-MSCs. Adipogenic differentiation capacity (Oil Red O staining), osteogenic differentiation capacity (Alizarin Red staining), and chondrogenic differentiation capacity (Alcian blue staining) (scale bar =250 μm) (n = 3).

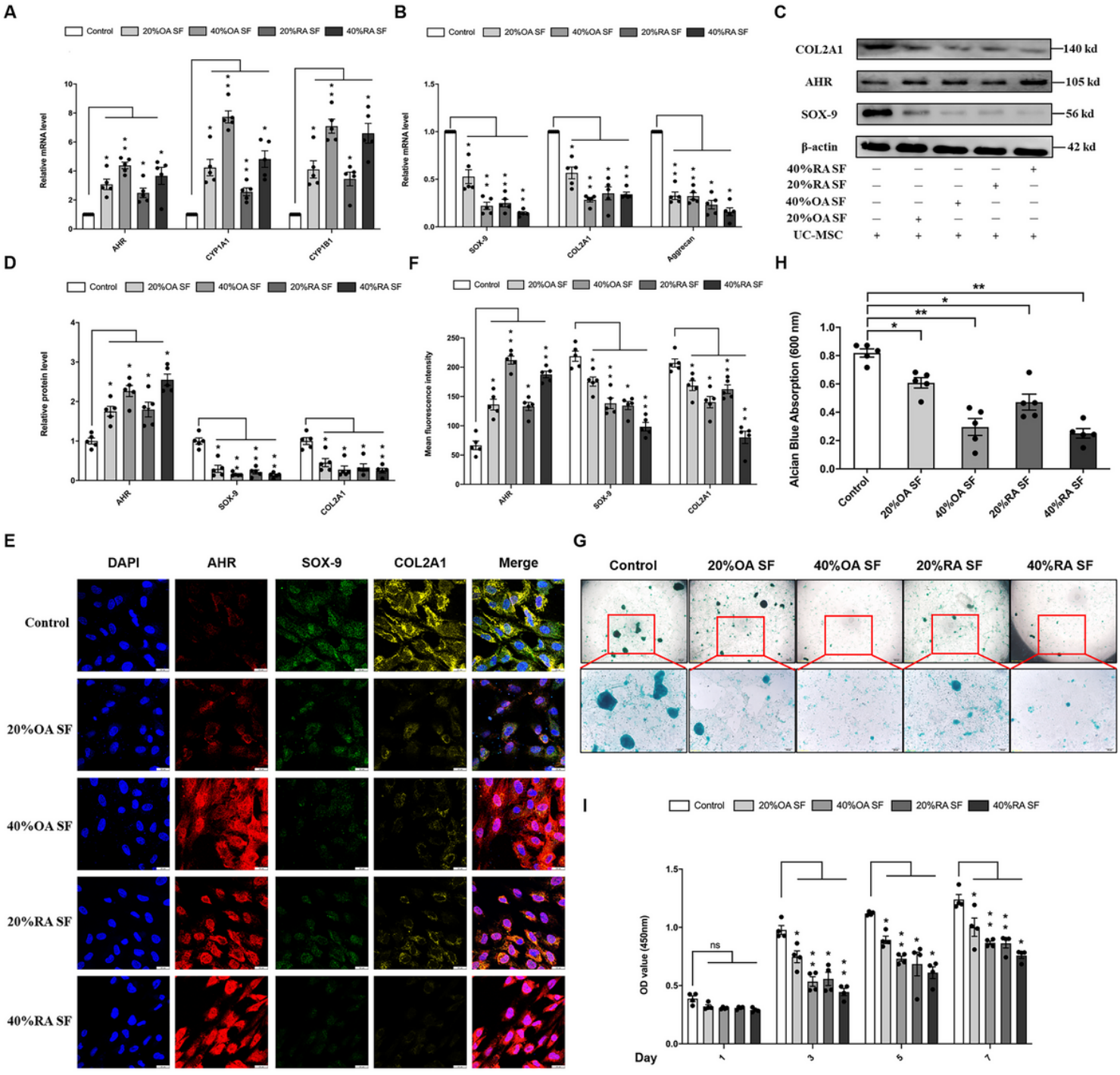

Figure 2

OA/RA SF activates AHR and inhibits the chondrogenesis and proliferation of UC-MSCs. A Relative mRNA expression of AHR, and downstream genes CYP1A1 and CYP1B1 at day 14 of chondrogenic differentiation (n = 5). **B** Relative mRNA expression of cartilage matrix genes SOX-9, COL2A1 and Aggrecan at day 14 of chondrogenic differentiation (n = 5). **C, D** Protein levels of AHR, COL2A1 and SOX9 were analyzed using western blotting at day 14 of chondrogenic differentiation, and their relative expression was normalized by β-actin (n = 5). **E, F** Expression and localization of AHR, SOX-9 and COL2A1 were detected by confocal immunofluorescence microscopy at day 14 of chondrogenic

differentiation, and the mean fluorescence intensity was quantified (scale bar = 25μm) (n = 5). **G**, **H** Alcian Blue staining for evaluating chondrogenic differentiation of UC-MSCs and the staning eluent was quantified (scale bar = 200μm, scale bar = 100μm) (n = 5). **I** The CCK-8 assay was used to detect the cell vitality of UC-MSCs treated with OA or RA SF for 1, 3, 5 and 7 days (n = 4). Each experiment was repeated 4-5 times independently, and the data was reported as mean ± SEM. $^{*}P < 0.05$, $^{**}P < 0.01$.

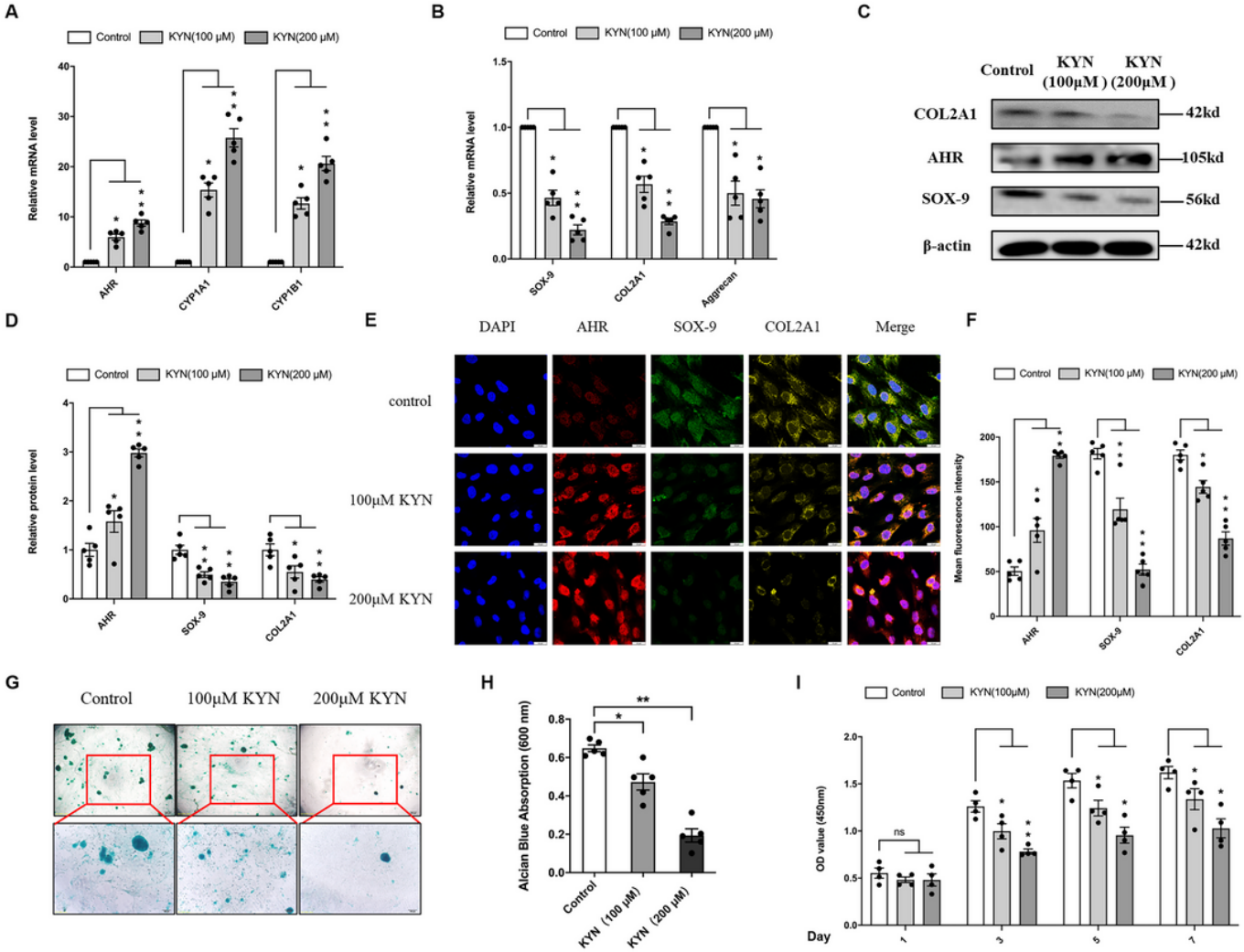

Figure 3

KYN-AHR axis activation suppressed the chondrogenic and proliferative activity of UC-MSCs. In the presence of chondrogenic medium, UC-MSCs were incubated with KYN (0, 100μM, or 200μM) for 14 days. **A** qRT-PCR assay was used to detect the mRNA expression level of AHR and its downstream target genes CYP1A, CYP1B1 (n = 5). **B** The mRNA expression level of chondrogenic markers SOX-9, COL2A1, and Aggrecan (n = 5). **C**, **D** The protein expression of AHR, SOX-9, and COL2A1 were detected by Western blot, and their relative expression was normalized by β-actin (n = 5). **E, F** The expression and location of AHR, SOX-9, and COL2A were detected using confocal microscopy (Scale bar = 25μm) (n = 5). **G**, **H** Alcian blue staining and relative quantitative analysis were used to evaluate the effects of KYN on the chondrogenic differiation of UC-MSCs (scale bar = 200μm, scale bar = 100μm) (n = 5). **I** The CCK-8 assay was used to

detect the cell vitality of UC-MSCs treated with KYN for 1, 3, 5 and 7 days (n = 4). Each experiment was repeated 4-5 times independently, and data were reported as mean ± SEM. $^{*}P < 0.05$, $^{**}P < 0.01$.

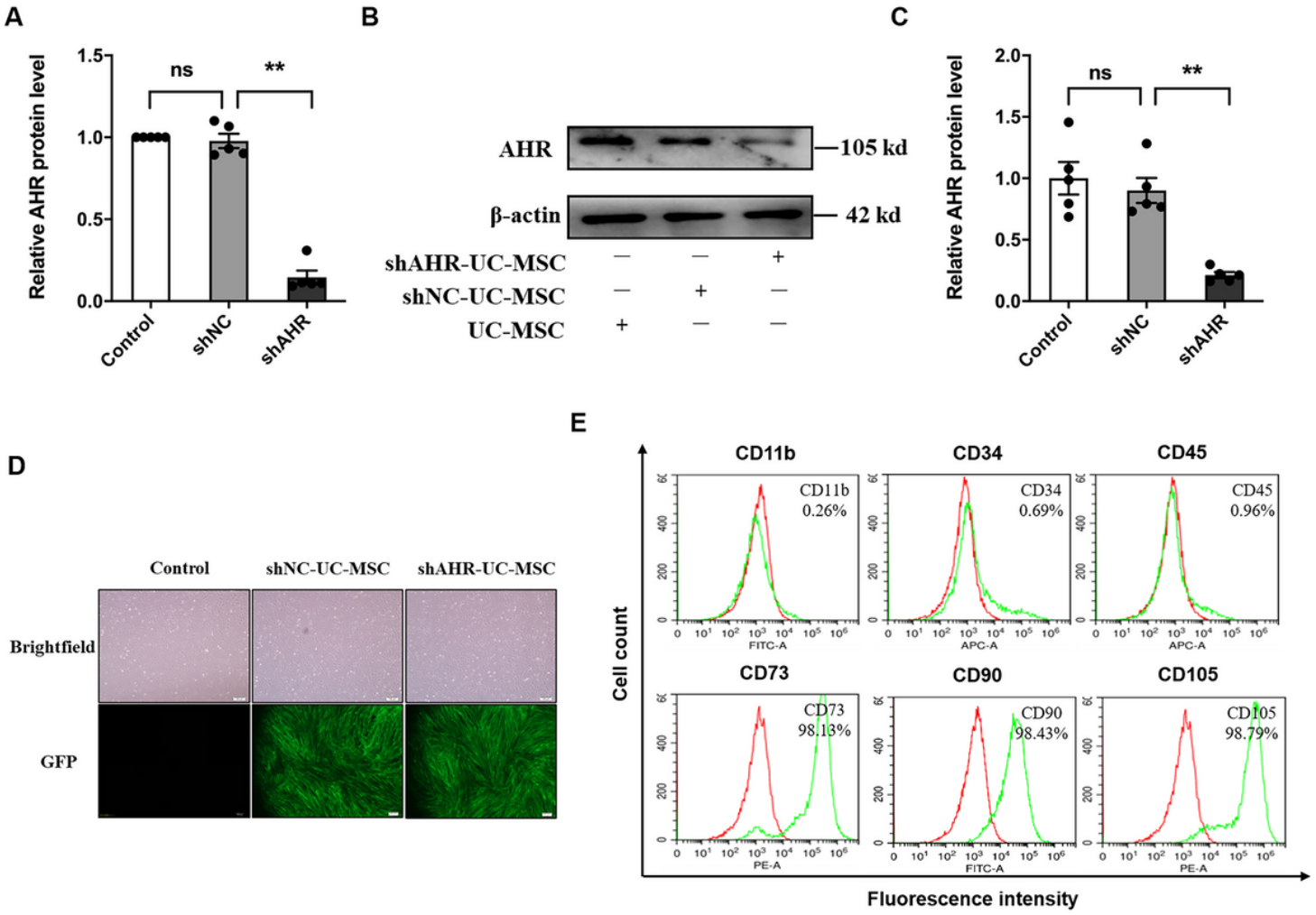

Figure 4

Lentiviral transfection to knockdown AHR in UC-MSCs. A Relative mRNA expression of AHR in control, shNC, and shAHR groups (n = 5). **B**, **C** Protein levels of AHR in the control, shNC, and shAHR groups (n = 5). **D** Images of GFP-positive UC-MSCs under a normal microscope and a fluorescence microscope (scale bar = 100 μm). **E** The phenotype identification of shAHR-UC-MSCs using flow cytometry (n = 3). The data are shown as mean ± SEM for triplicate. $^{*}P < 0.05$.

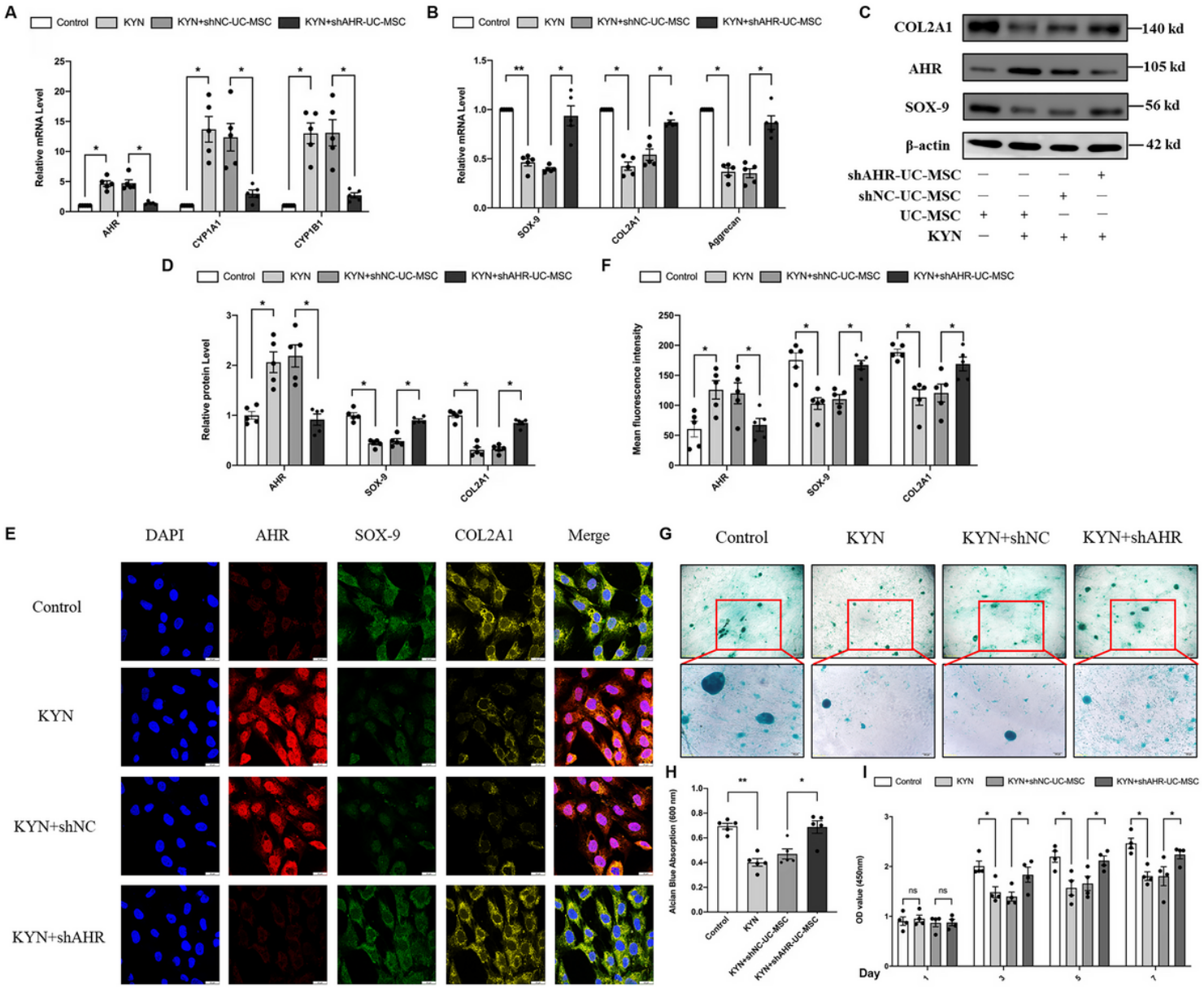

Figure 5

AHR knockdown reversed the inhibition effect of KYN treatment on chondrogenesis and proliferation of UC-MSCs. A, **B** AHR, CYP1A, CYP1B, SOX-9, COL2A1, and Aggrecan gene expression were evaluated by quantitative qRT-PCR (n = 5). **C**, **D** Western blot analysis of AHR, SOX-9, and COL2A1 protein level, and their relative expression was normalized by β-actin (n = 5). **E**, **F** immunofluorescent staining of AHR, SOX-9, and COL2A1 in UC-MSCs, and the mean fluorescence intensity was quantified (scale bar = 25μm) (n = 5). **G**, **H** Alcian blue staining (scale bar = 200μm, scale bar = 100μm) and quantification (n = 5). **I** The CCK-8 assay was used to detect the cell vitality of shAHR-UC-MSCs treated with KYN for 1, 3, 5 and 7 days (n = 4). Each experiment was repeated 4-5 times independently, and data was reported as mean ± SEM. $^{*}P < 0.05$, $^{**}P < 0.01$.

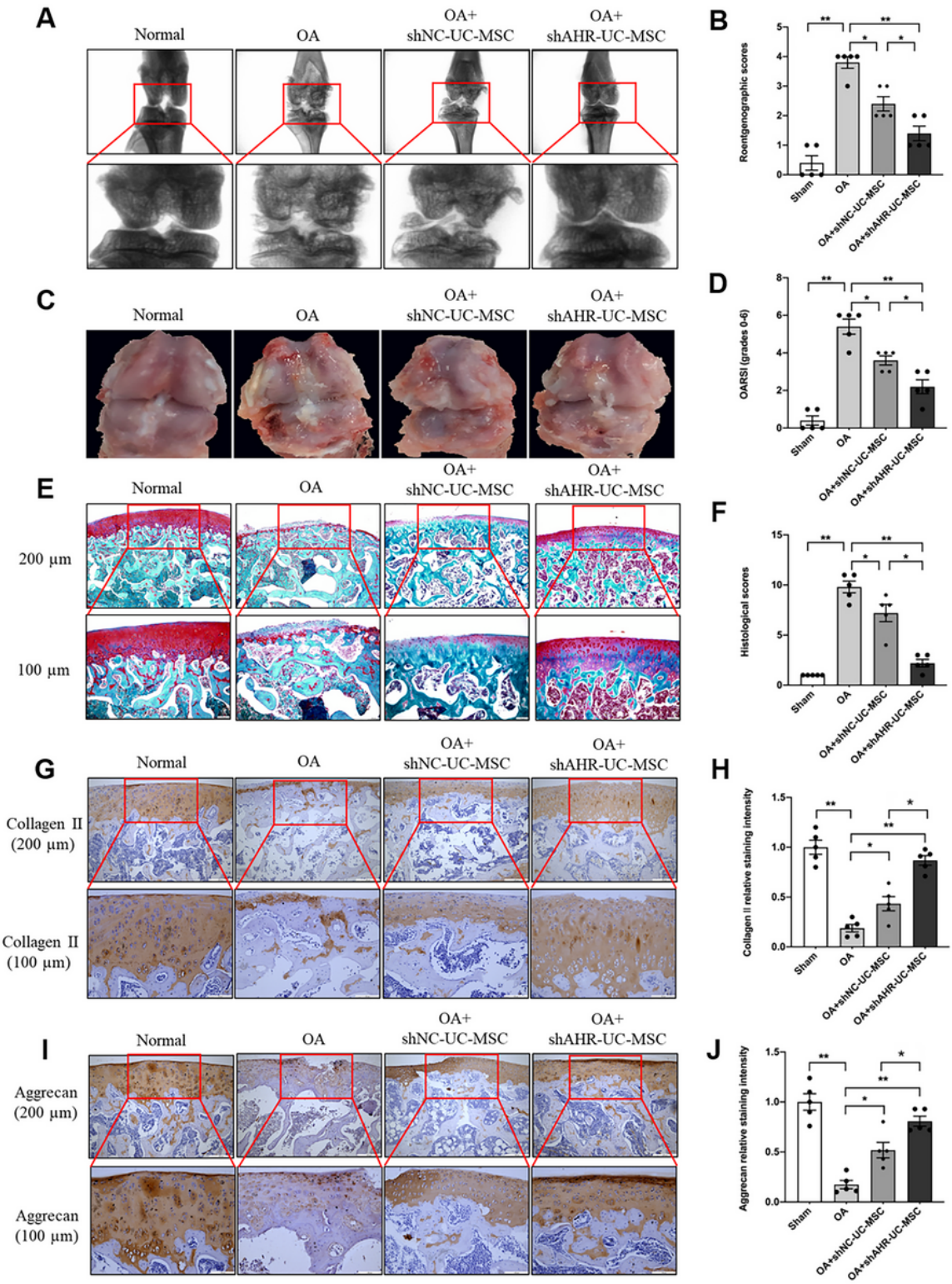

Figure 6

The effect of shAHR-UC-MSCs on cartilage protection in vivo. A, **B** X-Ray was used to evaluate the severity of OA in the knee joint before the animals were euthanized and the degree of cartilage lesions and osteophyte formation were assessed by the Kellgren-Lawrence scoring system (n = 5). **C**, **D** Gross morphology of articular cartilage damage of rats from different group, and cartilage destruction was evaluated using the OARSI scoring system (n = 5). **E**, **F** Safranin O-fast green staining for

histopathologically observing the articular cartilage damage of rats from different group, and Mankin's score was used to evaluate the degree of cartilage destruction (n = 5). **G-J** Immunohistochemical staining was used for assessing the expression of Collagen II and Aggrecan, and their quantitative analysis (n = 5). Data were expressed as means ± SEM. $^{*}P < 0.05$, $^{**}P < 0.01$.

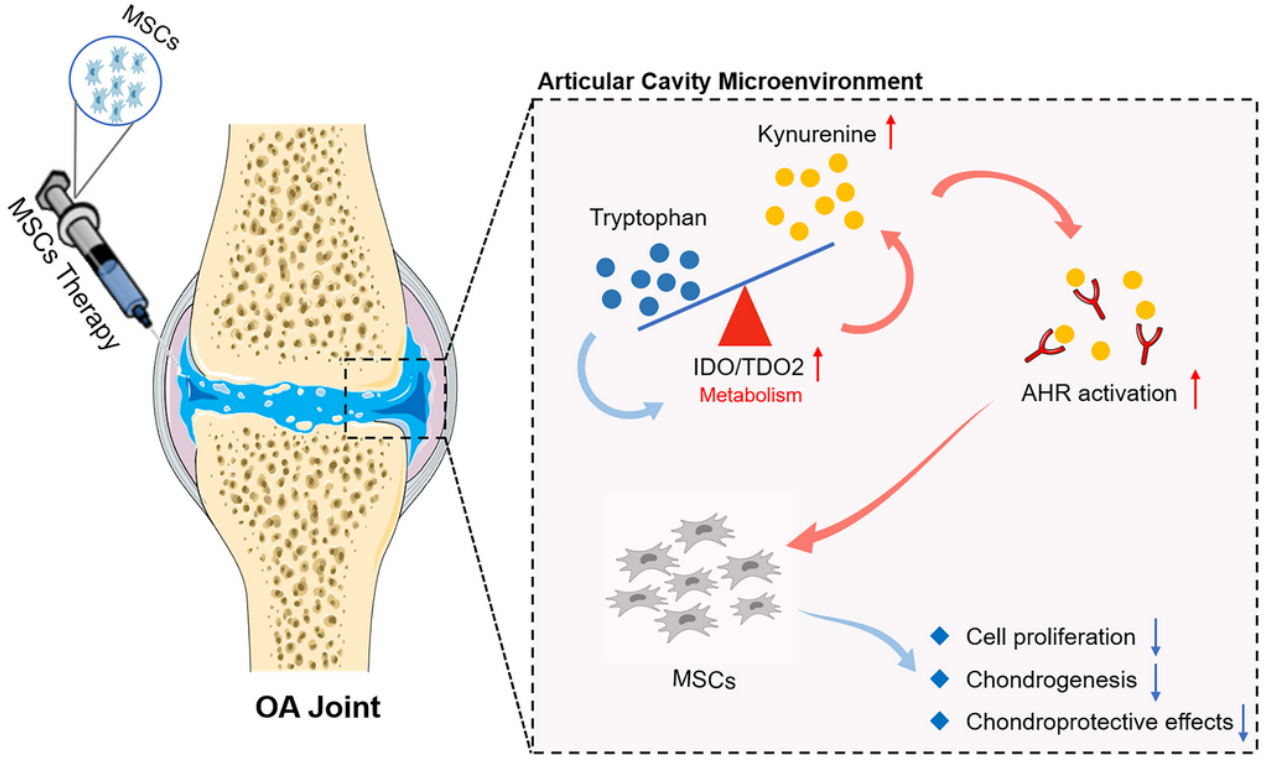

Figure 7

Activation of KYN-AHR axis impairs the chondrogenesis and chondroprotective effects of human umbilical cord-derived mesenchymal stem cells. KYN-AHR pathway on the chondrogenic and chondroprotective effects of UC-MSCs, which provided a theoretical basis for the clinical MSCs applications in the treatment of cartilage destruction diseases such as OA.

Supplementary Files

This is a list of supplementary files associated with this preprint. Click to download.

- Additionalfile1.pdf